Ionization Equilibria and Conformational Transitions in Polyprotic Molecules and Polyelectrolytes

Garces Gonzalez, José Luis; Koper, Ger J. M.; Borkovec, Michal

How to cite

GARCES GONZALEZ, José Luis, KOPER, Ger J. M., BORKOVEC, Michal. Ionization Equilibria and Conformational Transitions in Polyprotic Molecules and Polyelectrolytes. In: Journal of Physical Chemistry. B, Condensed Matter, Materials, Surfaces, Interfaces and Biophysical, 2006, vol. 110, n° 22, p. 10937–10950. doi: 10.1021/jp060684i

This publication URL: https://archive-ouverte.unige.ch/unige:145504
Publication DOI: 10.1021/jp060684i

Ionization Equilibria and Conformational Transitions in Polyprotic Molecules and Polyelectrolytes

José L. Garcés

Center of Theoretical Chemistry and Department of Physical Chemistry, Barcelona University, Martí i Franqués, 1, E-08028 Barcelona, Catalonia, Spain

Ger J. M. Koper

Department of Chemical Technology, Delft University of Technology, PO Box 5045, 2600 GA Delft, The Netherlands

Michal Borkovec*

Department of Inorganic, Analytical, and Applied Chemistry, University of Geneva, 30 Quai Ernest-Ansermet, 1211 Geneva 4, Switzerland

Received: February 1, 2006; In Final Form: April 3, 2006

The coupling between proton binding and conformational degrees of freedom in polyprotic molecules and polyelectrolytes is studied theoretically. Our approach combines the classical rotational isomeric state (RIS) model developed by Flory and the site binding (SB) model used to treat proton binding equilibria. The properties of the resulting SBRIS model, which treats conformational degrees of freedom and proton binding on equal footing, are studied with statistical mechanical techniques. Quantities of interest, such as titration curves, conformational probabilities, or macroscopic binding constants, are expressed as thermal averages and are evaluated by direct enumeration of states or by transfer matrix techniques. We further demonstrate that in the SBRIS model conformational degrees of freedom can be averaged out, leading to the contracted description within the SB model. In most cases, this contraction leads to higher order interactions, which may not be present at the SBRIS level (e.g., triplet interactions). Several examples are discussed to illustrate the concepts developed. The case of succinic acid exemplifies the situation in its simplest form. The model can further rationalize the very different titration behavior of poly(acrylic acid) (PAA) and poly(methacrylic acid) (PMAA). In particular, the characteristic "jump" in the titration curve of PMAA is described quantitatively and is interpreted in terms of a conformational transition.

Introduction

In the 1950s, Steiner,[1] Marcus,[2] and Katchalsky[3] have pioneered the understanding of the ionization process of weak polyelectrolytes. They introduced a site binding (SB) model, which defines the ionization state as a sequence of interacting sites, each of which characterized by its individual protonation state (i.e., protonated and deprotonated). The polyelectrolyte is then parametrized in terms of a microscopic ionization constant of the individual site and the pair interaction energies between neighboring sites. Coulombic interactions between the charged groups make the latter repulsive.[4,5] The necessary thermal averages can be evaluated with statistical mechanical techniques, including direct enumeration and Monte Carlo simulations. In the meantime, such SB models have been used widely to address titration curves obtained from potentiometry and nuclear magnetic resonance of polyprotic molecules, polyelectrolytes, and proteins.[5−10]

During the same period, Flory has developed the rotational isomeric state (RIS) model of polymeric chains.[11] This model treats a neutral polymeric chain as a sequence of interacting bonds, each of which is being characterized by a discrete set of rotational states (i.e., trans and two gauche conformations). The chain is then parametrized in terms of the (free) energies of the individual rotational states of the bonds, and the interaction energies between neighboring pairs of bonds. The interactions are usually repulsive, since they mainly originate from excluded volume interactions between side groups. On the basis of these assumptions, the necessary thermal averages can be evaluated with statistical mechanical techniques, mainly with transfer matrix methods. The RIS model has been successfully used to rationalize a wide range of physical properties of the individual chain, such as, its gyration radius, dipole moment, polarizability, and birefringence.[11−13]

Effects of coupling between ionization and conformation have been pointed out repeatedly for polyprotic molecules as well as for weak polyelectrolytes. One important illustration is the swelling of polyelectrolytes as they ionize. For example, poly(acrylic acid) (PAA) as well as poly(methacrylic acid) (PMAA) swell with increasing pH, as documented with viscosity measurements.[14,15] In the case of PAA, one observes a gradual swelling with increasing degree of ionization.[14] This trend was quantitatively reproduced by Monte Carlo simulations.[5] On the other hand, PMAA swells very suddenly at a particular degree of ionization and shows an unusual jump in the potentiometric titration curve.[15] This jump has been surmised to be driven by

* Corresponding author. Phone: +41 22 379 6405. Fax: + 41 22 379 6069. E-mail: michal.borkovec@unige.ch. Web: http://colloid.unige.ch/.

10.1021/jp060684i CCC: $33.50
Published on Web 05/16/2006

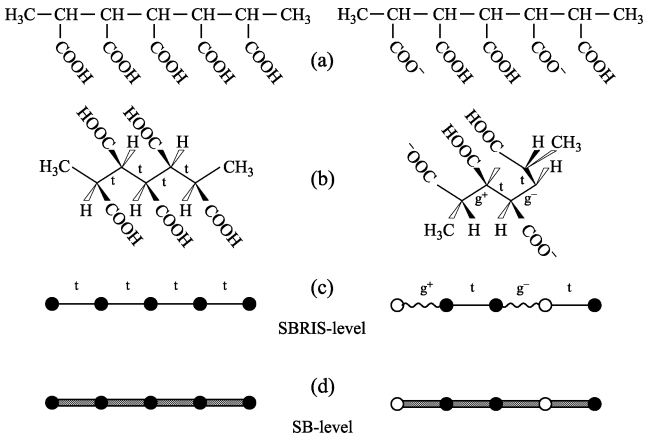

Figure 1. Schematic representation of the different levels of description for two different states of a hypothetical isotactic pentacarboxylic acid: (a) chemical formula; (b) conformational structures; (c) SBRIS-level description (rotomicrostate); (d) contracted SB-level description (microstate). Filled circle refers to a protonated site, and a open circle to a deprotonated site. A straight line represents a trans conformation and a wavy line one of the two gauche conformations.

attractive hydrophobic interactions between the methyl groups. Its resemblance to a first-order phase transition has attracted substantial attention among theorists.[16−18] A similar phenomenon is the helix−coil transition, which has been amply discussed in the biochemistry literature, particularly for poly(peptides).[20] The classical example is poly(L-glutamic acid), which shows a similar jump in the titration curve as PMAA.[21,22] The helix−coil transitions were interpreted in terms of an energy balance between repulsive electrostatic interactions and attractive hydrogen bonding, and they are ubiquitous in proteins and poly(saccharides).

The coupling between the ionization and conformational degrees of freedom has been further studied for diprotic and triprotic acids and bases.[23−26] All these studies conclude that the ionization process is normally accompanied by conformational changes. For example, for succinic acid it was shown that the gauche conformer is favored at low pH, while at high pH the trans conformer dominates.[23,24] Noszál et al.[27] have documented the pronounced conformational changes of amino acids as a function of pH. Thus, a specific protonation state of a molecule normally corresponds to a mixture of different conformers and is only rarely represented by a single conformer.

In this paper, we present a unified framework to address the coupling between the ionization and conformational degrees of freedom from the statistical mechanical point of view. We propose a discrete site-bond model, which is a combination of the SB and RIS models. The model will thus be referred to as the SBRIS model, and it treats proton binding on sites and discrete rotational states of the bonds on equal footing. The spirit of the model is summarized in Figure 1 with a hypothetical pentacarboxylic acid. The carboxyl groups can be protonated or deprotonated. This molecule can be in different conformations, depending on the rotational state of the carbon bonds along the chain. Two specific examples of protonation and conformational states are indicated in Figure 1b. When the protonation and conformational states of each site and bond are specified, one refers to a *rotomicrostate*.[27] The SBRIS model considers the ionization and conformational degrees of freedom as discrete variables, in terms of which each protonation and conformation state can be uniquely specified (see Figure 1c). On the basis of this description, we obtain detailed insight into the coupling between the ionization state and the molecular conformation, including small polyprotic acids or bases as well as weak polyelectrolytes.

We shall further discuss the consequences of averaging over the conformational degrees of freedom. In this situation, the conformations are no longer explicitly considered, and the molecular states are now specified by the protonation state of each group only (see Figure 1d). Such a state is commonly referred to as a *microstate*, while the so-called *macrostate* just specifies the total number of bound protons. From the averaging process, the classical SB model is recovered. However, the microscopic ionization constants and the interaction parameters entering the classical SB model are specific averages of the corresponding parameters over the different conformers. This averaging process may lead to multisite interactions, such as the triplet interactions, which were introduced on formal grounds earlier.[28] Another example of the emergence of interactions is the classical model of allosteric binding to proteins.[32,33] The classical model for hemoglobin comprises four noninteracting sites, and they are assumed to have different affinities in two different conformations. Due to the averaging over the conformational states, a cooperative interaction emerges. Many of our conclusions with be exemplified with the simplest SBRIS model, while we shall further discuss a more realistic SBRIS model for PAA and PMAA. It will be shown that the model can capture the behavior of both polyelectrolytes very well.

2. Site Binding (SB) Model of Protonation Equilibria

The protonation of a polyprotic molecule has been amply discussed within the framework of the site binding (SB) model.[1−4,6−10] For completeness, we provide a brief review of this model here.

Each ionizable site is labeled by an index $i = 1, ..., N$, where N is the total number of ionizable sites. The protonation state of each site is characterized by a variable s_i, which is chosen such that $s_i = 0$ when the site is deprotonated and $s_i = 1$ when it is protonated. The collection of state variables $s_1, ..., s_N$, abbreviated as s, uniquely specifies the protonation state of the molecule, commonly referred to as the *microstate*. The free energy of a polyprotic molecule $\tilde{F}(s)$ is commonly written as a cluster expansion

$$\frac{\beta\tilde{F}(s)}{\ln 10} = -\sum_i \mathrm{p}\tilde{K}_i s_i + \frac{1}{2!}\sum_{i,j}\tilde{\epsilon}_{ij}s_i s_j + \frac{1}{3!}\sum_{i,j,k}\tilde{\lambda}_{ijk}s_i s_j s_k + ... \quad (1)$$

which is conveniently defined in terms of the following dimensionless coefficients. The parameter $\mathrm{p}\tilde{K}_i = \log \tilde{K}_i$ is the common logarithm of the microscopic association constant of the site i given all other sites are deprotonated, $\tilde{\epsilon}_{ij}$ is the pair interaction parameter, while $\tilde{\lambda}_{ijk}$ values are the triplet interaction parameters. In most discussions, the triplet and higher order interactions are neglected, but they are sometimes necessary to achieve a proper description of proton binding. Their significance will be discussed below. Note that all these coefficients are invariant with respect to permutations of their subscripts, and they vanish whenever two of their indices are equal.

The associated semi-grand-canonical partition function reads

$$\tilde{\Xi} = \sum_s a_{\mathrm{H}}^n \, \mathrm{e}^{-\beta\tilde{F}(s)} \quad (2)$$

where a_{H} is the activity of protons related to $\mathrm{pH} = -\log a_{\mathrm{H}}$, $\beta^{-1} = k_{\mathrm{B}}T$ the thermal energy, and $n = \sum_i s_i$ is the total number of protons bound by the microstate s. The associated thermal average is

$$\langle ... \rangle = \sum_s \tilde{p}(s) \, ... \tag{3}$$

where the probability of an individual microstate is

$$\tilde{p}(s) = \tilde{\Xi}^{-1} a_{\mathrm{H}}^n \, \mathrm{e}^{-\beta \tilde{F}(s)} \tag{4}$$

An important thermal average is the degree of protonation

$$\theta = \frac{1}{N} \sum_{i=1}^{N} \langle s_i \rangle = \frac{a_{\mathrm{H}}}{N} \frac{\partial \ln \tilde{\Xi}}{\partial a_{\mathrm{H}}} \tag{5}$$

which can be measured by potentiometric titration.

For molecules with a finite number of sites, all states can be enumerated, and it is useful to expand the partition function in powers of the proton activity

$$\tilde{\Xi} = \sum_{n=0}^{N} \bar{K}_n a_{\mathrm{H}}^n \tag{6}$$

yielding the so-called binding polynomial.[6,32] The coefficients collect all terms of the partition function with a given number of bound protons, which are referred to as macrostates. They are commonly interpreted as the formation constants of a macrospecies and are related to the commonly reported macroscopic pK values by $\mathrm{p}\bar{K}_n = \log(\bar{K}_n/\bar{K}_{n-1})$. The macroconstants can be expressed in terms of the microconstants and the interaction parameters, namely

$$\bar{K}_1 = \sum_i \tilde{K}_i \tag{7}$$

with $\mathrm{p}\tilde{K}_i = +\log \tilde{K}_i$, then

$$\bar{K}_2 = \sum_{i>j} \tilde{K}_i \tilde{u}_{ij} \tag{8}$$

with $\tilde{\epsilon}_{ij} = -\log \tilde{u}_{ij}$ and

$$\bar{K}_3 = \sum_{i>j>k} \tilde{K}_i \tilde{K}_j \tilde{K}_k \tilde{u}_{ij} \tilde{u}_{jk} \tilde{u}_{ik} \tilde{w}_{ijk} \tag{9}$$

with $\tilde{\lambda}_{ij} = -\log \tilde{w}_{ij}$. The probability of a given microstate can be decomposed

$$\tilde{p}(s) = \tilde{\pi}_n(s) P_n(a_{\mathrm{H}}) \tag{10}$$

into $\tilde{\pi}_n(s)$ the conditional probability to find a microstate within a macrostate n, and the probability to find the macrostate n is

$$P_n(a_{\mathrm{H}}) = \tilde{\Xi}^{-1} \bar{K}_n a_{\mathrm{H}}^n \tag{11}$$

It is further customary to define microscopic constants for each site within a particular microstate, and these constants can be written as

$$\mathrm{p}\tilde{K}_i(s) = \mathrm{p}\tilde{K}_i - \sum_j \tilde{\epsilon}_{ij} s_j - \frac{1}{2} \sum_{j,k} \tilde{\lambda}_{ijk} s_j s_k - ... \tag{12}$$

The number of microstates is on the order of 2^N, and this number becomes enormous for a larger molecule. For this reason, the above quantities referring to individual microstates are no longer useful. However, the degree of protonation (cf. eq 5) remains well-defined and can be always evaluated by Monte Carlo simulations. For linear structures, thermal averages can also be found by transfer matrix techniques. The transfer matrix can be defined by introducing a restricted partition function

$$\tilde{\Xi}_{N'}(s'_{N'}) = \sum_s \mathrm{e}^{-\beta \tilde{F}(s)} \delta_{s'_{N'}, s_{N'}} \tag{13}$$

which is an ordinary partition function of a subchain with N' sites numbered from the left to the right and where the state of the last site is fixed to $s'_{N'} = 0$ or 1. In the case of nearest neighbor interactions, the partition function can be simply obtained through a recursion relation

$$\tilde{\Xi}_{N'} \mathbf{V} = \tilde{\Xi}_{N'+1} \tag{14}$$

where $\tilde{\Xi}_{N'}$ is a row vector with the elements $\tilde{\Xi}_{N'}(0)$ and $\tilde{\Xi}_{N'}(1)$ and $\mathbf{V}$ is the transfer matrix. We use Flory's convention, where the transfer matrix is applied to a row vector from right, and thereby adds a site and a bond to the chain in the same direction. The recursion relation is initiated with a suitably chosen initiating row vector $\mathbf{q}^{\mathrm{T}}$ and terminated by a column vector $\mathbf{p}$. The superscripted T denotes a transpose. Thus, the partition function of a chain with N identical sites can be written as

$$\tilde{\Xi} = \mathbf{q}^{\mathrm{T}} \mathbf{V}^N \mathbf{p} \tag{15}$$

For long chains, the partition function can be evaluated from the largest eigenvalue Λ of the transfer matrix

$$\tilde{\Xi} \sim \Lambda^N \tag{16}$$

from which the degree of protonation can be obtained by differentiation.

The archetypal case is the linear chain with nearest neighbor pair interactions. In this case, the transfer matrix reads

$$\mathbf{V} = \begin{bmatrix} 1 & z \\ 1 & uz \end{bmatrix} \tag{17}$$

where $z = Ka_{\mathrm{H}}$ is the reduced activity with $\log K = \mathrm{p}K$ representing the binding constant and $\epsilon = -\log u$ is the pair interaction parameter. The matrix can be read in the following fashion. The left column describes the effects of adding an empty site. In this case, the free energy does not change and the matrix elements are unity. Upon addition of an occupied site to an empty site, no pair interactions have to be considered, and the contribution to the partition function is z. When one adds an occupied site next to an occupied site, one must consider pair interactions as well, and the contribution is uz. The initiating and terminating vectors are $(1, 0)$ and $(1, 1)^{\mathrm{T}}$. When finite systems are considered, the binding constants of oligomers can be evaluated, while from the derivative of the largest eigenvalue, the titration curve of the infinite chain is found. This model is identical to the classical one-dimensional Ising model of a magnet.[30,31] When higher order interactions are present, transfer matrixes involving several sites are necessary, as discussed elsewhere.[29]

3. Rotational Isomeric State (RIS) Model of Conformational Equilibria

Let us now recall the basic notions of the rotational isomeric state (RIS) model of conformational degrees of freedom. More details can be found in Flory's monograph.[11]

Each chemical bond is labeled by an index $\alpha = 1, ..., M$ within a molecule containing M bonds. The discrete rotational state of each bond can be described by a state vector $\mathbf{c}_\alpha$ with a dimension corresponding to the number of states of the bond,

which is typically three, namely, trans, gauche$^+$, and gauche$^-$. The state $\mathbf{c}_\alpha$ vector contains zeros everywhere, except unity at the position of the actual rotational state. For example, the column vector $(1, 0, 0)^T$ represents a bond in the state trans, while $(0, 1, 0)^T$ refers to the state gauche$^+$. Thus, the collection of the state vectors $\mathbf{c}_1$, ..., $\mathbf{c}_M$ abbreviated as $\mathbf{c}$ specifies the conformational state of the molecule. The conformational free energy of a molecule can be also written as a cluster expansion

$$F_c(\mathbf{c}) = -\sum_\alpha \mathbf{f}_\alpha \cdot \mathbf{c}_\alpha + \frac{1}{2}\sum_{\alpha,\beta} \mathbf{H}_{\alpha\beta} : \mathbf{c}_\alpha \mathbf{c}_\beta + ... \qquad (18)$$

where $\mathbf{f}_\alpha$ is the coefficient vector of the free energies of the individual rotational states of the bond α and the matrix $\mathbf{H}_{\alpha\beta}$ contains the interaction energies among the different rotational states between bonds α and β. The symbols $\cdot$ and : denote the vector and matrix contraction, respectively. Higher order contributions have not been discussed so far. Note that the latter matrix is invariant upon exchange of α and β.

The partition function for the conformational degrees of freedom reads

$$\Xi_c = \sum_{\mathbf{c}} e^{-\beta F_c(\mathbf{c})}$$

with the associated thermal average

$$\langle ... \rangle_c = \sum_{\mathbf{c}} p_c(\mathbf{c}) ... \qquad (20)$$

where the probability of a given conformation is

$$p_c(\mathbf{c}) = \Xi_c^{-1} e^{-\beta F_c(\mathbf{c})} \qquad (21)$$

Flory was discussing numerous thermal averages.[11] The simplest example of those is the fraction of a given conformational state, represented here as a vector

$$\boldsymbol{\gamma} = \frac{1}{M}\sum_{\alpha=1}^{M} \langle \mathbf{c}_\alpha \rangle \qquad (22)$$

where M is the number of bonds affecting the conformational state of the molecule.

For linear chains, one can again employ the transfer matrix technique to evaluate the partition function. For a symmetric aliphatic carbon chain with rotational states t, g$^+$, and g$^-$, Flory has introduced the transfer matrix

$$\mathbf{U} = \begin{bmatrix} 1 & \sigma & \sigma \\ 1 & \sigma\psi & \sigma\omega \\ 1 & \sigma\omega & \sigma\psi \end{bmatrix} \qquad (23)$$

where $-kT \ln \sigma = f$ is the free energy of either gauche state with respect to the trans state, given all other bonds are also trans. The parameters ψ and ω characterize the nearest neighbor pair interactions between bonds. Thereby, $-kT \ln \psi = H_{++} = H_{--}$ represents the pair interaction energy of two consecutive g$^+$ or g$^-$ conformations, and $-kT \ln \omega = H_{+-} = H_{-+}$ of two consecutive g$^+$ and g$^-$ conformations, or vice versa.

For a symmetric chain, both gauche states can be combined into one, and the model can be mapped exactly onto a model with two states t and g. The corresponding transfer matrix reads

$$\mathbf{U} = \begin{bmatrix} 1 & g \\ 1 & gh \end{bmatrix} \qquad (24)$$

where $g = 2\sigma$ is the statistical weight of the gauche state and $h = (\psi + \omega)/2$ is the statistical weight of the pair interactions. The interpretation of this matrix is identical to the above case of proton binding. Since the trans bond is taken as reference, adding this bond does not change the free energy. Adding a gauche bond to a trans one leads to a contribution of its statistical weight, and two consecutive gauche bonds also include the pair interaction energy. The initiating and terminating vectors contain the elements (1, 0) and (1, 1). Again, this model is identical to the one-dimensional Ising chain.[30,31]

4. Protonation and Conformation Acting Together

A molecule in a specific protonation and conformational state can be characterized by the state variables s and $\mathbf{c}$. This state will be referred to as a *rotomicrostate*. Since the different conformers are independent species, one can apply the same ideas as developed in section 2 to each conformer separately. The free energy of an ionizable molecule has been expressed within the SB model as a cluster expansion in terms of the state variables s (cf. eq 1). Since each conformational state $\mathbf{c}$ is independent, the same form holds for each conformation separately, namely

$$\frac{\beta F_p(s,\mathbf{c})}{\ln 10} = -\sum_i p\hat{K}_i(\mathbf{c}) s_i + \frac{1}{2!}\sum_{i,j} \epsilon_{ij}(\mathbf{c}) s_i s_j + \frac{1}{3!}\sum_{i,j,k} \lambda_{ijk}(\mathbf{c}) s_i s_j s_k - ... \qquad (25)$$

where we have assumed that the coefficients can be different for the different configurations $\mathbf{c}$. The reference state of this free energy is the fully deprotonated state of each conformer, but the conformers might differ in their free energies as well. This contribution can be described by the RIS model expression given in eq 18. The total free energy of the molecule is thus given by the sum

$$F(s,\mathbf{c}) = F_c(\mathbf{c}) + F_p(s,\mathbf{c}) \qquad (26)$$

where the deprotonated molecule with all bonds in the trans state is used as the reference state for the conformations. Depending on the situation, other reference states might be useful. This free energy is the basis of the SBRIS model introduced here. Of course, this splitting of the free energy is arbitrary. Alternatively, one could bind the protons first, and then consider the conformation. However, we find the present representation more intuitive.

So far, we have not specified the dependencies of the coefficients entering eq 25 on the conformations $\mathbf{c}$. Two approaches can be adopted. The first approach is to consider a set of coefficients $pK_i(\mathbf{c})$, $\epsilon_{ij}(\mathbf{c})$, and eventually $\lambda_{ijk}(\mathbf{c})$ for each conformational state $\mathbf{c}$. This approach is useful for small molecules with a limited number of conformational states. For larger molecules, however, the number of conformational states is very large, and one would have to deal with an overwhelming number of parameters. For this reason, an alternative approach is to keep only terms to a given order in s and $\mathbf{c}$ in the free energy.

Let us discuss the expansion to third order. Since terms involving the binding constants $p\hat{K}_i(\mathbf{c})$ are linear in the protonation state variables s_i, we have to consider terms in $\mathbf{c}_\alpha$ to second order, namely

$$p\hat{K}_i(\mathbf{c}) = pK_i^{(0)} + \sum_\alpha \mathbf{m}_i^{(\alpha)} \cdot \mathbf{c}_\alpha + \sum_{\alpha\beta} \boldsymbol{\Delta}_i^{(\alpha\beta)} : \mathbf{c}_\alpha \mathbf{c}_\beta \qquad (27)$$

whereby we have introduced the microconstant $pK_i^{(0)}$ of the fully

deprotonated state in an all-trans configuration, a vector $\mathbf{m}_i^{(\alpha)}$, and the matrix $\mathbf{\Delta}_i^{(\alpha\beta)}$, which is symmetric upon exchange of the coefficients α and β and vanishes when these coefficients are equal. The vector $\mathbf{m}_i^{(\alpha)}$ describes the shift of the chemical potential of site *i* upon change in the rotational state of bond α and will be referred to as *conformational shift parameters*. The matrix $\mathbf{\Delta}_i^{(\alpha\beta)}$ describes the correction to this shift due to rotational state of bonds α and β and thus will be referred to as *shift correction parameters*. The pair interaction energies are quadratic in s_i. Since terms up to third order are being considered, only linear correction terms have to be taken into account

$$\epsilon_{ij}(\mathbf{c}) = \epsilon_{ij}^{(0)} + \sum_{\alpha} \mathbf{d}_{ij}^{(\alpha)} \cdot \mathbf{c}_{\alpha} \tag{28}$$

The elements of the coefficient vector $\mathbf{d}_{ij}^{(\alpha)}$ will be referred to as the *pair coupling parameters*, and they represent the change in the interaction energy between sites *i* and *j* upon change in the rotational state of bond α. This quantity is symmetric in α and β and also vanishes when these coefficients are equal. The fact that $\mathbf{d}_{ij}^{(\alpha)}$ do not vanish probably represents the main reason for the coupling between proton binding and conformations. For this reason, terms of at least third order must be kept in the free energy expansion. The triplet interactions are already third order in s_i and thus can be assumed to be constants

$$\lambda_{ijk}(\mathbf{c}) = \lambda_{ijk}^{(0)} \tag{29}$$

For the matter of completeness, we should mention that the cluster expansion to third order also does include triplet interaction between the bonds, which would be described by a third rank coefficient tensor entering eq 18. However, for the matter of simplicity, this tensor will not be invoked here. The above expansions introduce three important parameters responsible for coupling between the protonation and conformational degrees of freedom within the SBRIS model, namely, the conformational shift parameters, shift correction parameters, and pair coupling parameters. To third order, no other parameters are necessary.

As soon as the free energy $F(s,\mathbf{c})$ has been specified, one can evaluate the semi-grand partition function in the classical way as

$$\Xi = \sum_{s,\mathbf{c}} a_{\mathrm{H}}^{n} \mathrm{e}^{-\beta F(s,\mathbf{c})} \tag{30}$$

where the associated thermal average is

$$\langle ... \rangle = \sum_{s,\mathbf{c}} p(s,\mathbf{c}) \, ... \tag{31}$$

with the probability of a conformational microstate

$$p(s,\mathbf{c}) = \Xi^{-1} a_{\mathrm{H}}^{n} \mathrm{e}^{-\beta F(s,\mathbf{c})} \tag{32}$$

where *n* is the number of protons bound by the microstate. The average degree of protonation can be expressed as

$$\theta = \frac{1}{N} \sum_{i=1}^{N} \langle s_i \rangle = \frac{a_{\mathrm{H}}}{N} \frac{\partial \ln \Xi}{\partial a_{\mathrm{H}}} \tag{33}$$

while elements of the vector

$$\boldsymbol{\gamma} = \frac{1}{M} \sum_{\alpha=1}^{N} \langle \mathbf{c}_{\alpha} \rangle \tag{34}$$

represent the fraction of bonds in a given rotational state.

4.1. Macrostates, Microstates, and Rotomicrostates. For systems with a small number of sites, it is useful to enumerate the macrostates and microstates. Recall that for a *macrostate* only the total number of protons is fixed, while for a *microstate* the protonation state of each individual site is fixed. When conformations and protonation are treated explicitly, one considers the *rotomicrostates*. Thereby, for the protonation state of each individual site also the rotational state of each bond is specified. One could also discuss other possibilities of defining similar states, for example, where the total number of protons and the rotational states are fixed or where only the rotational states are specified, but we will not discuss these alternatives here.

The probabilities of a given rotomicrostate can be again split into

$$p(s,\mathbf{c}) = \pi_n(s,\mathbf{c}) P_n(a_{\mathrm{H}}) \tag{35}$$

where $\pi_n(s,\mathbf{c})$ is the conditional probability of a rotomicrostate within a macrostate *n* and $P_n(a_{\mathrm{H}})$ the macrostate probability (cf. eq 11). We can further resolve the conditional probability as

$$\pi_n(s,\mathbf{c}) = \pi_n^{(\mathbf{c})}(s) \rho_n(\mathbf{c}) \tag{36}$$

where $\pi_n^{(\mathbf{c})}$ is the conditional probability to find a certain protonation state *s* for a given conformation $\mathbf{c}$ and macrostate *n* and

$$\rho_n(\mathbf{c}) = \bar{K}_n^{-1} \sum_{s} \mathrm{e}^{-\beta F(s,\mathbf{c})} \delta_{n,\sum s_i} \tag{37}$$

is the probability to find the conformation $\mathbf{c}$ within a macrostate. Summing eq 36 over all conformations, we find

$$\tilde{\pi}_n(s) = \sum_{\mathbf{c}} \pi_n^{(\mathbf{c})}(s) \rho_n(\mathbf{c}) \tag{38}$$

Thus, the important consequence of this equation is that each microstate can be decomposed into contributions of different rotomicrostates. In other words, a microstate is a collection of rotomicrostates, quite in analogy to the fact that a macrostate is a collection of microstates. Finally, we observe that the probability to find a certain conformation can be written as

$$\boldsymbol{\gamma}(\mathbf{c}) = \frac{1}{N} \sum_{n=0}^{N} \rho_n(\mathbf{c}) P_n(a_{\mathrm{H}}) \tag{39}$$

and its pH dependence is given by the macrostate probabilities.

4.2. Transfer Matrices. The partition functions can be again directly enumerated or evaluated with the transfer matrix technique. On the SBRIS level, the transfer matrix is constructed easily. One simply has to consider the supermatrix consisting of four submatrixes, namely, describing the addition of a bond and a site $\mathbf{U}_{00}$, $\mathbf{U}_{01}$, $\mathbf{U}_{10}$, and $\mathbf{U}_{11}$, which consider addition of a deprotonated site to a deprotonated site, a deprotonated site to a protonated site, a protonated site to a deprotonated site, and a protonated to a protonated site, respectively. Thus, the overall transfer matrix reads

$$\mathbf{V} = \begin{bmatrix} \mathbf{U}_{00} & \mathbf{U}_{01} \\ \mathbf{U}_{10} & \mathbf{U}_{11} \end{bmatrix} = \begin{bmatrix} \mathbf{U} & \mathbf{U}*\mathbf{z} \\ \mathbf{U} & \mathbf{U}*\mathbf{z}*\mathbf{u} \end{bmatrix} \tag{40}$$

where **U** is the Flory matrix describing the conformations (cf. eq 23), **z** the reduced activity matrix, and **u** the pair interaction matrix. The term-by-term product matrix $\mathbf{C} = \mathbf{A}*\mathbf{B}$ is defined by its elements $c_{ij} = a_{ij}b_{ij}$. The elements of the activity matrix are given by $z_{\alpha\beta} = \hat{K}_{\alpha\beta}a_{\mathrm{H}}$ where $\hat{K}_{\alpha\beta}$ is the affinity constant of the corresponding conformation, while the elements of the pair interaction matrix $u_{\alpha\beta}$ denote the proton−proton interactions in the particular conformations. If the chains are not isotactic, or multiple bonds link the ionizable sites, a sequence of different transfer matrixes must be considered. The arguments follow exactly the discussion by Flory.[11] Illustrative examples will be given below.

4.3. Contracting Conformational Degrees of Freedom. In section 2 we have summarized the SB model of proton binding, where no conformational degrees of freedom were considered. Obviously, when the conformational degrees of freedom are averaged out from the SBRIS model, one must obtain the SB model. In particular, one can express the parameters entering the free energy of the SB model (cf. eq 1) from the more general SBRIS free energy (cf. eq 26). For this correspondence to be valid, the partition function given in eq 2 must obey the equivalence

$$\Xi = \Xi_{\mathrm{c}}\tilde{\Xi} \tag{41}$$

where Ξ_{c} is given by eq 19. Substituting eq 26 into eq 19, the partition function can be expressed as a conformational average

$$\tilde{\Xi} = \sum_{s} a_{\mathrm{H}}^{n} \langle \mathrm{e}^{-\beta F_{\mathrm{p}}(s,\mathbf{c})} \rangle_{\mathrm{c}} \tag{42}$$

where $n = \sum_i s_i$ and the conformational averages are defined in eq 20. They have to be carried out over the chosen reference state, defined here as the deprotonated state. We thus find the important correspondence

$$\mathrm{e}^{-\beta\tilde{F}(s)} = \langle \mathrm{e}^{-\beta F_{\mathrm{p}}(s,\mathbf{c})} \rangle_{\mathrm{c}} \tag{43}$$

Inserting eqs 1 and 25 and collecting powers in K_i, we find that the binding constants in the contracted system are given by

$$\tilde{K}_i = \langle \hat{K}_i(\mathbf{c}) \rangle_{\mathrm{c}} \tag{44}$$

The pair interaction energies can be expressed as

$$\tilde{u}_{ij} = \frac{\langle \hat{K}_i(\mathbf{c})\hat{K}_j(\mathbf{c})u_{ij}(\mathbf{c}) \rangle_{\mathrm{c}}}{\tilde{K}_i\tilde{K}_j}$$

where $u_{ij}(\mathbf{c})$ and $\tilde{u}_{ij}$ are defined by the relations $\epsilon_{ij}(\mathbf{c}) = -\log u_{ij}(\mathbf{c})$ and $\tilde{\epsilon}_{ij} = -\log \tilde{u}_{ij}$. The triplet interaction energies can be found as

$$\tilde{w}_{ijk} = \frac{\langle \hat{K}_i(\mathbf{c})\hat{K}_j(\mathbf{c})\hat{K}_k(\mathbf{c})u_{ij}(\mathbf{c})u_{jk}(\mathbf{c})u_{ik}(\mathbf{c})w_{ijk}(\mathbf{c}) \rangle_{\mathrm{c}}}{\tilde{K}_i\tilde{K}_j\tilde{K}_k\tilde{u}_{ij}\tilde{u}_{jk}\tilde{u}_{ik}} \tag{46}$$

with $\lambda_{ijk}(\mathbf{c}) = -\log w_{ijk}(\mathbf{c})$ and $\tilde{\lambda}_{ijk}(\mathbf{c}) = -\log \tilde{w}_{ijk}$. The expansion can be continued, and in the general case, higher order interactions are recovered. Once these parameters are known, the macroconstants can be calculated from eqs 7−9.

While the application of these expressions will be discussed in the later sections, several important observations can be already made here. First, the parameters of the contracted free energy can be indeed expressed in terms of the conformation-dependent parameters. However, the correspondence is not simple, and given by eqs 44, 45, and 46. Second, even when the cluster expansion of the SBRIS model terminates, the cluster expansion of the SB model does generally not. For example, one can obtain triplet interactions in the SB model even when no such interactions have been be considered in the SBRIS model. In general, it will not be possible to represent the system on the SB level exactly, as higher order interactions will be present in the general case. However, one surmises that the higher order contributions will be small, and in most cases the cluster expansion is expected to converge rapidly. Only few coefficients should be sufficient to represent the system to good accuracy.

Naturally, it would also be possible to average over the binding degrees of freedom and obtain a contracted RIS model. In this case, however, the effective parameters entering the RIS become pH dependent. This approach will not be considered here.

5. Simplest Four-State SBRIS Model

Let us now illustrate the present concepts with a four-state SBRIS model on a linear chain. In our opinion, this is the simplest nontrivial model to combine effects of proton binding and conformational degrees of freedom on a unified level.

Consider two protonation states for each site (protonated and deprotonated) and two conformational states (trans and gauche). When only nearest neighbor pair interactions are considered, these states can be now described with a single 4 × 4 transfer matrix, which is a combination of the corresponding two 2 × 2 matrixes corresponding to the SB or RIS models. Taking the general structure indicated in eq 40, and the corresponding submatrixes given in eqs 17 and 24, we obtain

$$\mathbf{U} = \begin{bmatrix} 1 & g & z_{\mathrm{tt}} & gz_{\mathrm{tg}} \\ 1 & gh & z_{\mathrm{tg}} & ghz_{\mathrm{gg}} \\ 1 & g & z_{\mathrm{tt}}u_{\mathrm{t}} & gz_{\mathrm{tg}}u_{\mathrm{t}} \\ 1 & gh & z_{\mathrm{tg}}u_{\mathrm{g}} & ghz_{\mathrm{gg}}u_{\mathrm{g}} \end{bmatrix} \tag{47}$$

where $z_{\alpha\beta} = \hat{K}_{\alpha\beta}a_{\mathrm{H}}$ are the reduced site activities and u_α the corresponding parameters which depend on the conformation of the neighboring bonds on the left (α = t, g) and on the right (β = t, g). The initiating and terminating vectors are $(1, g, z_{\mathrm{t}}, gz_{\mathrm{g}})$ and $(1 + z_{\mathrm{t}}, 1 + z_{\mathrm{g}}, 1 + z_{\mathrm{t}}u_{\mathrm{t}}, 1 + z_{\mathrm{g}}u_{\mathrm{g}})^{\mathrm{T}}$. The reduced site activities for the terminal sites are $z_\alpha = \hat{K}_\alpha a_{\mathrm{H}}$, since they depend only on the state of one bond. As will be discussed in the following, this model can mimic many features characterizing the coupling of conformations and ionizations for oligomers and linear polyelectrolytes. Often, much more complicated situations can be mapped onto this simple four-state SBRIS model on a linear chain. One example will be given in section 6.

5.1. Emergence of Cooperativity. The simplest nontrivial case is the dimer. While this situation is easily analyzed and has been amply discussed in the literature,[6,23,24,32,33] let us briefly discuss how it emerges from the present SBRIS formalism.

The dimer consists of two sites and a single bond, and for this reason bond−bond interactions do not enter. An example is succinic acid, where two carboxylic groups are attached to two carbon atoms. For simplicity, let us assume that both sites are equivalent and that two conformational states trans (t) and gauche (g) have to be considered. For each conformation, we thus consider the affinity constants $\mathrm{p}\hat{K}_{\mathrm{t}}$ and $\mathrm{p}\hat{K}_{\mathrm{g}}$ and the pair interaction parameters ϵ_{t} and ϵ_{g}, respectively. Applying the contraction formula eq 44, the microscopic binding constant reads

$$\tilde{K} = \frac{\hat{K}_t + g\hat{K}_g}{1+g} \tag{48}$$

where g is the statistical weight of the trans conformation. The microscopic interaction parameter becomes (cf. eq 45)

$$\tilde{u} = \frac{(\hat{K}_{t2}u_t + g\hat{K}_{g2}u_g)(1+g)}{(\hat{K}_t + g\hat{K}_g)^2} \tag{49}$$

Normally, we parametrize the situation by the microscopic constant $p\tilde{K} = \log \tilde{K}$ and the pair interaction parameter $\tilde{\epsilon} = -\log \tilde{u}$. On the contracted SB level, these two parameters describe the situation exactly. On the macroscopic level, the formation constants follow from eqs 7 and 8 to be

$$\bar{K}_1 = 2\tilde{K} \tag{50}$$

and

$$\bar{K}_2 = \tilde{K}^2\tilde{u} \tag{51}$$

From these macroconstants, the titration curve can be obtained. The probabilities of the different conformations can also be found.

The statistical weight g controls which conformation is the predominant one. For $g = 0$, it is trans conformation, while the gauche conformation dominates if $g \to \infty$. In either extreme case, only one conformation governs the behavior, and the apparent parameters are given through the ones of the corresponding conformer. In the intermediate situation, both conformers play a role, and two different scenarios can be distinguished.

The first scenario is encountered when the binding constants are comparable, namely, when $p\hat{K}_t \simeq p\hat{K}_g$. In this case, the effective interaction parameter $\tilde{\epsilon}$ varies monotonically from ϵ_t to ϵ_g as the statistical weight g is being increased. This scenario is the most common one and will be illustrated with succinic acid in section 6.

The second scenario arises when the binding constants are sufficiently different, namely, when $p\hat{K}_t \gg p\hat{K}_g$ or $p\hat{K}_t \ll p\hat{K}_g$. While the limiting value of the effective interaction parameter $\tilde{\epsilon}$ is still ϵ_t for $g = 0$ and ϵ_g for $g \to \infty$, its dependence is nonmonotonic and $\tilde{\epsilon}$ passes through a minimum, leading to attractive (cooperative) interactions. Recall the archetypical case of two independent sites ($\epsilon_t = \epsilon_g = 0$) for illustration. When the binding constants are equal ($p\hat{K}_t = p\hat{K}_g$), there are no effective interactions and $\tilde{\epsilon} = 0$. When $p\hat{K}_t \neq p\hat{K}_g$ the interaction parameter becomes negative and goes through a minimum as a function of g. Thus, one obtains cooperative interactions on the microscopic level.

Take $p\hat{K}_t = 4$ and $p\hat{K}_g = 6$ as an example. The minimum value of $\tilde{\epsilon} \simeq -1.40$ occurs at $g = 100$. At this point, the effect of cooperativity is most pronounced. The corresponding titration curves are shown in Figure 2a. The titration curve undergoes a relatively steep transition between the limiting cases of the titration curves in the trans and the gauche state. The titration curve is steeper than that for a single site, indicating positive cooperativity.

The conformational transition is more clearly apparent in Figure 2b, where the conformational probabilities are shown. Figure 2c illustrates the macrostate probabilities as a function of pH, which are characterized by the macroconstants $p\bar{K}_1 \simeq 4.60$ for the first protonation step, and $p\bar{K}_2 \simeq 5.40$ for the second protonation step. Due to the cooperativity effect, these constants are in the reverse order to the usual sequence, and the probability

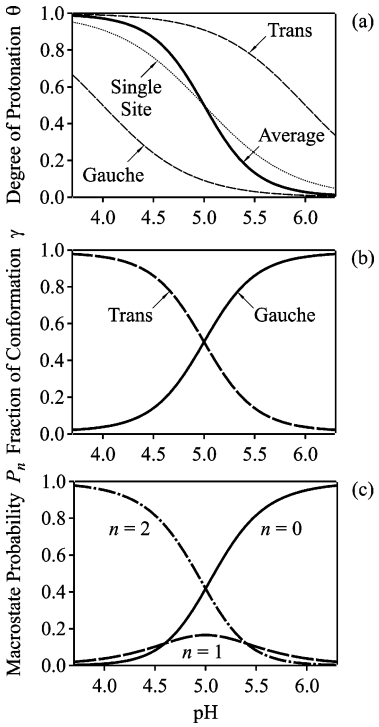

Figure 2. Properties of a symmetric diprotic acid or base as a function of pH. There are no interactions ($\epsilon_t = \epsilon_g = 0$) but a strong dependence of the binding constant upon conformation ($p\hat{K}_t = 4$ and $p\hat{K}_g = 6$). The conformational weight $g = 100$ leads to apparent cooperativity ($\tilde{\epsilon} \simeq -1.40$). (a) The average degree of protonation θ compared with the corresponding quantities for each conformer and a single site. (b) Conformer probabilities γ. (c) Macrostate probabilities P_n.

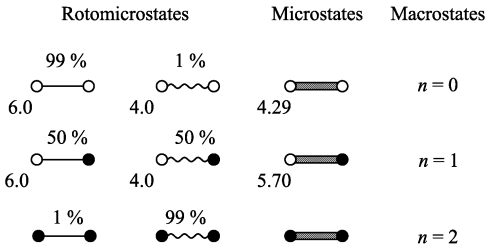

Figure 3. Rotomicrostates, microstates, and macrostates of a symmetric diprotic acid or base. The probabilities and microscopic pK values are indicated. The macrostates specify the number of protons bound (n = 0, 1, 2). There are no interactions ($\epsilon_t = \epsilon_g = 0$) but a strong dependence of the binding constant upon conformation ($p\hat{K}_t = 4$ and $p\hat{K}_g = 6$). The conformational weight $g = 100$ leads to apparent cooperativity ($\tilde{\epsilon} \simeq -1.40$). The parameters are the same as in Figure 2.

of the singly protonated macrostate remains <17%. Figure 3 shows the probabilities of the individual conformational microstates and the corresponding microconstants. Similar effects were discussed in more detail for substituted succinic acids, and the nature of the conformation transition strongly depends indeed on the nature of the substituents and their interactions.[24]

This cooperativity effect is the simplest illustration of the famous allosteric effect, discussed amply in the biochemistry literature.[32,33] This mechanism explains the strong cooperativity of oxygen binding by hemoglobin. The allosteric effect occurs always, if the affinities of the binding sites depend on the conformational state, and tends to diminish effective pair interactions. It becomes more pronounced with the larger number of sites. We shall encounter a similar phenomenon in our discussion of polyelectrolytes.

5.2. Emergence of Triplet Interactions. As a second example, consider a linear molecule with two bonds and three

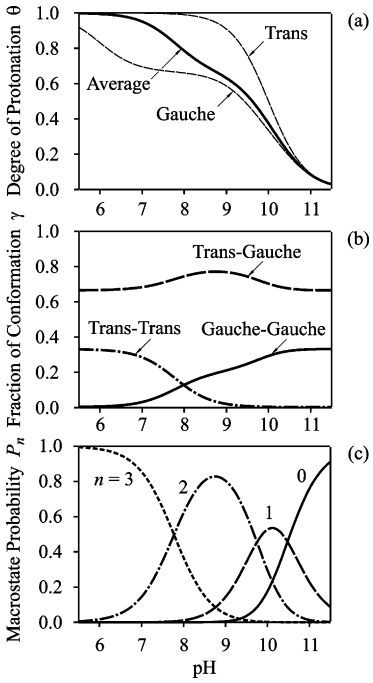

Figure 4. Properties of a linear triprotic acid or base as a function of pH. The sites are equivalent and there is a strong dependence of the pair interactions upon conformation ($p\hat{K} = 10$, $\epsilon_t = 0$, and $\epsilon_g = 2$). The conformational equilibria are characterized by $g = 100$ and $h = 0.01$. (a) Degree of protonation together with the results, when the molecules is constrained to all-gauche or all-trans conformations, (b) fractions of conformation, and (c) macrostate probabilities.

ionizable sites. The triprotic situation will illustrate another important effect, namely, the emergence of triplet interactions. For simplicity, let us assume that the binding constants are all the same and independent of the conformation. However, we suppose that the pair interactions do depend on the conformation and assume different values, ϵ_t and ϵ_g, in the trans and gauche state, respectively. Again we apply the contraction formulas and obtain the cluster parameters of the contracted SB model. For the pair interactions we have

$$\tilde{u} = \frac{(1+g)u_t + g(1+gh)u_g}{1+2g+g^2h} \tag{52}$$

where g is the weight of the gauche conformation and h is the Boltzmann factor describing the interactions between the bonds. The triplet interactions turn out to be

$$\tilde{w} = \frac{(u_t^2 + 2gu_tu_g + g^2hu_g^2)(1+2g+g^2h)}{[(1+g)u_t + g(1+gh)u_g]^2} \tag{53}$$

which we usually parametrize as $\tilde{\lambda} = -\log \tilde{w}$. Very similar relations were proposed by Ben-Naim.[25]

In the case of $\epsilon_t \neq \epsilon_g$ and $h \neq 1$, the model predicts nonvanishing triplet interactions for intermediate values of the conformational weight g. To illustrate the role of repulsive triplet interactions, consider a hypothetical linear triprotic molecule characterized by a protonation constant independent of the conformational state $p\hat{K} = 10$, with interaction parameters $\epsilon_t = 0$ and $\epsilon_g = 2$. The proton binding isotherms of these two conformations are compared with the actual isotherm, which involves the conformational equilibria characterized by $g = 100$ and $h = 0.01$, in Figure 4a. In basic conditions, the molecule is preferentially in the gauche conformation, while in acidic

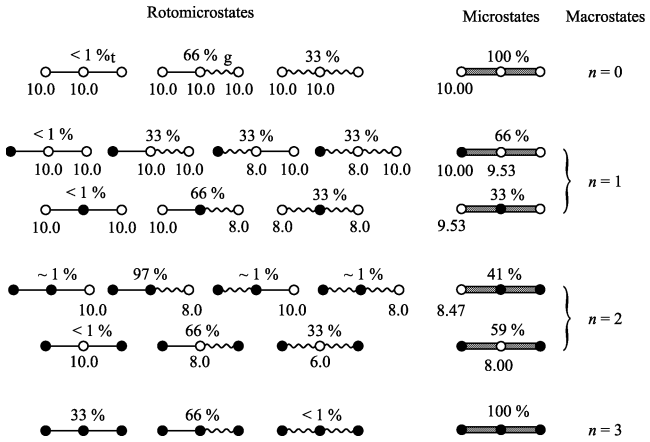

Figure 5. Rotomicrostates, microstates, and macrostates of a linear triprotic acid or base. The probabilities and microscopic pK values are indicated. The macrostates specify the number of protons bound ($n = 0, 1, 2, 3$). The sites are equivalent and there is a strong dependence of the pair interactions upon conformation ($p\hat{K} = 10$, $\epsilon_t = 0$, and $\epsilon_g = 2$). The conformational equilibria are characterized by $g = 100$ and $h = 0.01$. The parameters are the same as in Figure 4.

conditions the molecule adopts preferentially a trans configuration (see Figure 4b).

The situation can be interpreted on different levels. On the macroscopic level, the molecule is characterized by the macroconstants $p\bar{K}_1 \simeq 10.48$, $p\bar{K}_2 \simeq 9.75$, $p\bar{K}_2 \simeq 7.77$. The corresponding macrostate probabilities are shown in Figure 4c. If one considers the microscopic SB level, where the conformational degrees of freedom are averaged out, the equilibria are characterized by a microconstant $p\tilde{K} = 10$, and a pair and triplet interaction parameters of $\tilde{\epsilon} \simeq 0.47$ and $\tilde{\lambda} \simeq 1.07$. The corresponding probabilities and protonation constants of the microstates are shown in Figure 5.

The detailed SBRIS level of description concerns the different rotomicrostates summarized in Figure 5. The characteristic feature is the prominent doubly protonated state of 97%, where two neighboring protonated sites favor a trans bond, which in turn diminishes the repulsive interactions. To protonate this species, a repulsive interaction must be overcome. A similar enhancement of interactions occurs for the other prominent doubly protonated species, where the central site is not protonated. It can be again only protonated by overcoming the repulsive interaction of the gauche bond. This type of enhancement of mutual interactions is due to the presence of conformational degrees of freedom, and leads to the emergence of triplet interactions.

5.3. Conformational Transitions in Polyelectrolytes. Consider an infinite linear chain with sites connected by bonds and nearest neighbor interactions as described by the four-state SBRIS model (cf. eq 24). In this situation, the chain properties can be obtained by the maximum eigenvalue method. Illustrative results are summarized in Figure 6, where the top row shows the titration curves, and the bottom row the conformational probabilities. In all cases, we use an affinity constant of pK = 9, which is independent of the conformation of the bonds, and pair interaction parameters $\epsilon_t = 1$ and $\epsilon_g = 3$. This situation mimics the behavior of a weak polybase. Titration curves of an all-trans chain ($g = 0$) and an all-gauche chain ($g \to \infty$) are the same for all situations, and the actual titration curve must necessarily lie between these two extremes. While in some situations, one conformation may govern the behavior; in others, a conformational transition may occur during the titration. The nature of this transition depends strongly on the bond−bond

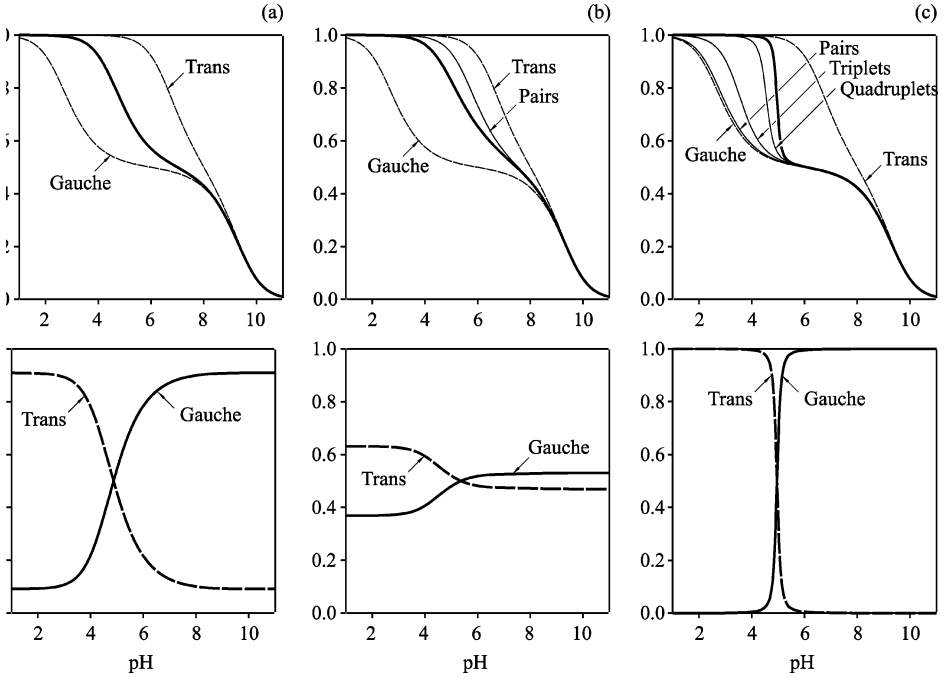

Figure 6. Linear infinite polyacid or polybase with equivalent sites with an affinity constant of $p\hat{K} = 9$, which is independent of the conformation of the bonds, and pair interaction parameters $\epsilon_t = 1$ and $\epsilon_g = 3$. Degree of protonation (top) and conformational probabilities (bottom). Dashed lines correspond to the titration curves of the all-gauche and all-trans conformation. Predictions of the four-state SBRIS model (thick solid lines) are compared to the successive approximations on the contracted SB level including pair, triplet, and quadruplet interactions (thin lines). The strength of bond−bond interactions is varied. (a) No interactions ($h = 1$ and $g = 10$) where the contracted SB description is exact on the pair level with $\tilde{\epsilon} = 2$. (b) Repulsive interactions ($h = 0.3$ and $g = 10$) where the contracted SB description coincides at the triplet level with the exact result on the scale of the graph ($\tilde{\epsilon} \simeq 1.46$, $\tilde{\lambda} \simeq 0.24$, $\tilde{\nu} = -0.01$) (c) Attractive interactions ($g = 0.1$ and $h = 100$) where the contracted SB description does not even coincide with the exact result at the quadruplet level ($\tilde{\epsilon} \simeq 2.95$, $\tilde{\lambda} \simeq -0.29$, and $\tilde{\nu} \simeq -0.47$).

interactions, and typical results for no interactions, repulsive interactions, and attractive interactions are shown in Figure 6. Let us discuss these three situations in more detail.

Consider first the case of no bond−bond interactions ($h = 1$, Figure 6a). The result of the four-state SBRIS model for $g = 10$ is shown. As the pH is decreased, the polyelectrolyte undergoes a conformation transition from an coiled state dominated by gauche bonds to an extended state dominated by trans bonds. Correspondingly, the titration curve of the polyelectrolyte initially follows the all-gauche chain, but as the chain undergoes the conformational transition, it swings toward the titration curve of the all-trans chain. However, the transition is very gradual, and the resulting titration curve remains between these two extremes.

How well does the contracted SB model describe the situation? In the case of no interaction between the bonds ($h = 1$), a remarkable result is found. Provided that the condition $\hat{K}_{tg} = (\hat{K}_{tt}\hat{K}_{gg})^{1/2}$ is satisfied, the cluster expansion of the contracted SB model terminates after the pair interaction term. This condition corresponds to the case where the shift correction parameters vanish (cf. eq 27). The model can be thus contracted *exactly* to the two-state SB model described by the transfer matrix given in eq 17. The effective interaction parameters can be expressed as follows. The effective binding constant is

$$\tilde{K} = \frac{(\hat{K}_{tt}^{1/2} + g\hat{K}_{gg}^{1/2})^2}{(1+g)^2} \tag{54}$$

and the effective pair interaction parameter

$$\tilde{u} = \frac{(u_t\hat{K}_{tt} + gu_g\hat{K}_{gg})(1+g)}{(\hat{K}_t^{1/2} + g\hat{K}_g^{1/2})^2} \tag{55}$$

As an illustration, take the common affinity constant $p\hat{K} = 9$ and the pair interaction parameters $\epsilon_t = 1$ and $\epsilon_g = 3$. The statistical weight of the trans state is $g = 10$, and there are no interactions between the bonds ($h = 1$). Figure 6a shows the result. We find the same effective binding constant $p\tilde{K} = 9$ and effective pair interaction parameter $\tilde{\epsilon} = 2$. The curve calculated with the contracted model coincides with the SBRIS result exactly.

When repulsive bond−bond interactions are present, the qualitative features remain similar to the previous case. Consider the same parameters describing the protonation, but take $g = 10$ and $h = 0.3$. The result is shown in Figure 6b. The conformational transition is now more gradual, and the resulting titration curve lies again between the two extremes of the all-trans and the all-gauche chain. However, in contrast to the case of no interactions, the resulting titration curve now becomes asymmetric.

In the presence of bond interactions, the cluster expansion on the contracted SB model no longer terminates but may converge rapidly. To assess the quality of this approximation, we have to evaluate the effective interaction parameters. The resulting expressions are given in the Appendix. An interesting aspect of this analysis is that for the four-state SBRIS model, all resulting cluster parameters are of the nearest neighbor type. Thus, the only nonvanishing pair interactions are between neighboring pairs of sites, only triplet interactions between neighboring triplets of sites, etc. For example, no next nearest neighbor pair interactions emerge. A similar observation was already made by analyzing titration data of linear polyamines.[7,28] For the repulsive case shown in Figure 6b we find the effective binding constant $p\tilde{K} = 9$ unchanged. On the other hand, the effective pair interaction parameter becomes $\tilde{\epsilon} \simeq 1.46$, and for the triplets we have $\tilde{\lambda} \simeq 0.24$, and for quadruplets $\tilde{\nu} \simeq -0.01$.

The successive approximations, on the pair, triplet, and quadruplet level, are shown in Figure 6b, and we observe that including the triplet interaction parameter suffices to describe the result of the SBRIS model accurately.

For attractive bond−bond interactions, even the qualitative features turn out to be quite different. Consider now the case of $g = 0.1$ and $h = 100$. The result is shown in Figure 6c. In this case, the conformational transition from gauche to trans is very sudden, and happens near pH 5.0. Correspondingly, the resulting titration curve follows the curve for the all-gauche chain at high pH, and then flips suddenly to the curve of the all-trans chain at low pH. Therefore, one almost observes a "jump" in the titration curve. Note that within this "jump" the curve remains continuous, and a discontinuity results only in the limit $h \rightarrow \infty$.

The validity of the contracted model can be again addressed by evaluating the effective interaction parameters (see Appendix). For the attractive case shown in Figure 6c, we find the effective binding constant $p\tilde{K} = 9$ again unchanged. The effective pair interaction parameter is $\tilde{\epsilon} \simeq 2.95$, for the triplets we have $\tilde{\lambda} \simeq -0.29$, and for quadruplets $\tilde{\nu} \simeq -0.47$. The successive approximations are again shown in Figure 6c. In this case, however, even the consideration of quadruplets does not lead to an acceptable description of the actual titration curve. Similar jumps in the titration curves were observed for poly(peptides), poly(L-glutamic acid) being the classical example.[20−22] They have been interpreted as conformational transitions within the chain.

The important point to realize is that a conformational transition might not be necessarily reflected in the titration curve. The most striking manifestation is that the simple four-state SBRIS model without bond−bond interactions is exactly equivalent to the two-state SB model, but nevertheless important conformation changes might take place. In the presence of bond−bond interactions, conformational changes might be more obvious in the titration curve, for example, though a "jump" or indirectly through its asymmetry (i.e., triplet interactions).

6. Illustrations

This section will illustrate the applicability of the SBRIS model with realistic systems. The aim is to give examples that illustrate the coupling between conformational and ionization degrees of freedom and demonstrate that the SBRIS model is able to capture these effects on a semiquantitative level. The more realistic case of three conformational states developed by Flory[11] will be used, and the appropriate configurations within the chain will be treated. Since the examples chosen will be all polycarboxylic acids, it is helpful to use the fully protonated chain as reference. The microscopic constants are then expressed with respect to the fully protonated state. Extensive comparisons with experimental data are beyond the scope of this paper.

6.1. Succinic Acid and Its Analogues. Succinic acid is a diprotic acid shown in Figure 7. Figueirido et al.[23] have used molecular dynamics simulations to estimate the interaction energies for the trans and gauche conformers to $\epsilon_t = 0.5$ and $\epsilon_g = 3.5$. These authors have further surmised equal microconstants of $p\hat{K} = 4.5$ for both conformers in the protonated state and a corresponding probability of 0.35 for the trans conformation.

The titration curve is illustrated in Figure 7a. The actual titration curve lies between hypothetical curves of both conformers. At high pH the molecule is exclusively in the trans state in order to minimize its energy caused by the strong repulsion of both charged groups. As the pH is increased, the gauche state becomes more prominent. Since we deal with a

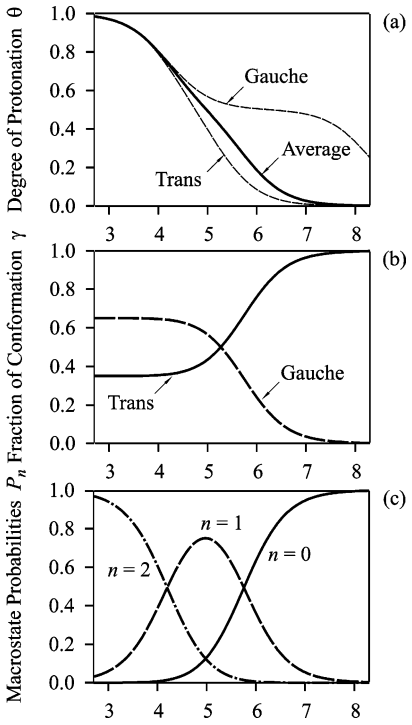

Figure 7. Conformational transition of succinic acid as a function of pH: (a) averaged degree of protonation compared to the hypothetical titration curves of the trans and gauche conformers; (b) fraction of each conformer; (c) macrostate probabilities.

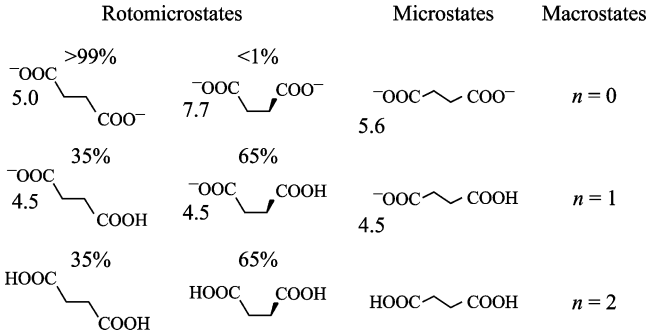

Figure 8. Rotomicrostates, microstates, and macrostates of succinic acid. The probabilities of the corresponding conformational microstates and the microconstants are indicated.

diprotic acid, the contracted model is exact (see Figure 7b). It gives a microconstant of 4.5 as before and an effective interaction parameter of $\epsilon_t = 0.96$. The macroconstants turn out to be $p\bar{K}_2 = 5.76$ and $p\bar{K}_1 = 4.20$ within this model. Figure 7c illustrates the relative populations of the different macrostates ($n = 0$, 1 and 2). The corresponding microstates are shown in Figure 8. The deprotonated species consists almost exclusively of the trans conformer.

The substantial difference between the interaction parameters in both conformers of the succinic acid is further supported with the parameters of fumaric (trans) and maleic (cis) acids, which are 0.8 and 3.7, respectively.[6] Ben-Naim has further discussed a series of substituted succinic acids, which also show substantial splitting of the ionization constants for the meso and racemic forms.[24] We suspect that these differences are largely attributable to the substantially different statistical weights of the respective conformations in the two different forms.

6.2. Poly(methacrylic acid) (PMAA) and Poly(acrylic acid) (PAA). The charge of polycarboxylic acids increases with increasing pH, and at the same time the molecules swell progressively. This behavior is summarized in Figure 6. While

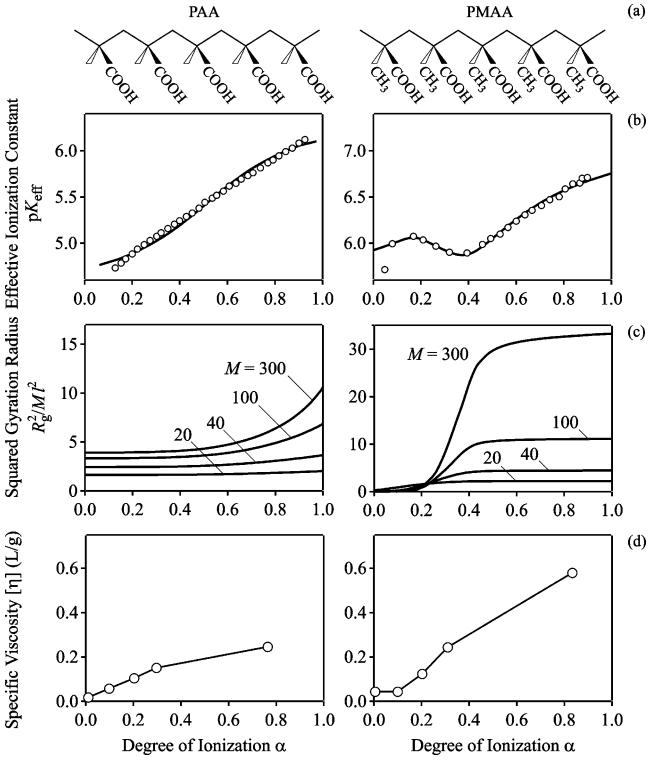

Figure 9. Behavior of poly(acrylic acid) (PAA) and poly(methacrylic acid) (PMAA) as a function of the degree of ionization α. Points represent experimental values and solid lines are calculated with the SBRIS model with values given in Table 1. (a) Structural formulas of the isotactic forms. (b) Titration curves represented as effective ionization constant pK_{eff} (cf. eq 56). Calculations are compared with the experimental data for isotactic PAA[35] and PMAA.[34] (c) Calculated square of the dimensionless gyration radius for different number of bonds *M*. (d) Experimental values of the specific viscosities [η] for PAA and PMMA.[14] The solid line serves to guide the eye.

poly(acrylic acid) (PAA) extends with increasing pH continuously, poly(methacrylic acid) (PMAA) swells substantially in an abrupt fashion within a narrow pH range. This behavior is illustrated in Figure 9c, where literature data for the specific viscosities for isotactic PAA and PMAA are shown.[14,15] The specific viscosity [η] (Staudinger index) is related to the size of a polymer coil.[11] It increases for PMAA abruptly near pH 6.5, while PAA features only a modest and continuous increase. This marked difference is due to the presence of methyl groups on the aliphatic backbone of PMAA.

The titration data for PAA and PMAA are shown in Figure 9b. As customary in polyelectrolyte literature, they are plotted as the effective ionization constant

$$\text{p}K_{\text{eff}} = \text{p}H + \log \frac{1-\alpha}{\alpha} \tag{56}$$

as a function of the degree of ionization $\alpha = 1 - \theta$. In the case of no interactions, it leads to a constant value of pK_{eff}. For interacting systems, pK_{eff} typically increased with increasing degree of ionization, as the presence of dissociated sites facilitate the dissociation of the remaining ones. While the titration data for isotactic PAA illustrate this trend nicely, an unusual feature is observed for PMAA (see Figure 9b). At a high degree of protonation, the apparent ionization constant pK_{eff} decreases as expected; at intermediate values they attain a plateau and finally decrease close to full protonation. The characteristic hump corresponds to a "jump" in the titration curve and signals an abrupt change in the molecular conformation. The viscosity data confirm these features.

To describe PAA and PMAA with the SBRIS model, two 6 × 6 transfer matrixes are necessary. They result directly from the classical Flory model of the asymmetric vinyl chain (section 4, chapter 6, ref 11). The first matrix adds a carbon bond and a CH_2 group to the carbon carrying with the carboxyl group and introduces the activities of the carboxyl groups, namely

$$\mathbf{U}_1 = \begin{bmatrix} \eta & 1 & \tau & 0 & 0 & 0 \\ \eta & 1 & \tau\omega & 0 & 0 & 0 \\ \eta & \omega & \tau & 0 & 0 & 0 \\ 0 & 0 & 0 & \eta z_{\text{tt}} & z_{\text{tg}} & \tau z_{\text{tg}} \\ 0 & 0 & 0 & \eta z_{\text{tg}} & z_{\text{gg}} & \tau\omega z_{\text{gg}} \\ 0 & 0 & 0 & \eta z_{\text{tg}} & \omega z_{\text{gg}} & \tau z_{\text{gg}} \end{bmatrix} \tag{57}$$

where $z_{\alpha\beta} = K_{\alpha\beta}a_{\text{H}}$ are the reduced site activities. The upper left 3 × 3 submatrix corresponds to the RIS matrix for the chain with uncharged carboxyl groups, referred to as the *d*-dyad by Flory.[11] The parameters η and τ are the Boltzmann factors corresponding to the trans and gauche$^-$ states, whereby the gauche$^+$ state is taken as reference. We further assume that the affinity constants are the same whenever the bonds are in any gauche state and that $K_{\alpha\beta} = (K_{\alpha\alpha}K_{\beta\beta})^{1/2}$. The latter condition means that the shift correction parameters (cf. eq 27) are neglected. The second matrix adds a carbon bond and a carbon with the carboxyl group to the CH_2 group, and introduces the pair interactions, namely

$$\mathbf{U}_2 = \begin{bmatrix} \eta\omega'\sigma u' & 0 & 0 & \eta\omega'\sigma & 0 & 0 \\ 0 & 0 & \omega\sigma u & 0 & 0 & \omega\sigma \\ 0 & \tau\omega\omega' u & 0 & 0 & \tau\omega\omega' & 0 \\ \eta\omega'\sigma & 0 & 0 & \eta\omega'\sigma & 0 & 0 \\ 0 & 0 & \omega\sigma & 0 & 0 & \omega\sigma \\ 0 & \tau\omega\omega' & 0 & 0 & \tau\omega\omega' & 0 \end{bmatrix} \tag{58}$$

The lower left 3 × 3 submatrix correspond to the RIS matrix for the uncharged carboxyl group, referred to as *dd*-dyad by Flory.[11] The reason the pair interaction parameters appear in the upper left corner of the matrix is because the protonated state is chosen as the reference state for the RIS model, and thus the carboxylic groups interact in their deprotonated state. The parameters η and τ are again the Boltzmann factors corresponding to the trans and gauche$^+$ states, while this time the gauche$^-$ state is taken as reference. The pair interactions are further assumed to be equal to $\epsilon = -\log u$ except when the two bonds are in the trans state, where the value is $\epsilon' = -\log u'$. When defining these matrixes, we focus on isotactic molecules for simplicity, as depicted in Figure 9a. Other tacticities can be handled within the same framework but will not be discussed here. However, the effects of tacticity are not extremely important for PAA analogues.

We assume the Boltzmann factors for the bond−bond interactions to vanish, whenever a carboxylic group points to the same direction as a hydrogen, methyl group, or the carbon atom of the backbone. These interactions are expected to be repulsive. The other interactions, which may be attractive, are summarized in Table 1. They are estimated from the molecular structure or fitting the titration data. For both polyelectrolytes, PAA and PMAA, the parameter ω' accounts for the formation of a hydrogen bond between two consecutive carboxylic groups pointing to the same direction, and its value has been estimated from typical hydrogen bond energies.[36]

The titration curves can be obtained by means of the discussed matrix methods, and they are compared in Figure 9 with the

TABLE 1: Conformational Parameters in the RIS Model for Protonated Isotactic PAA and PMAA

groups[a]	factor	PAA	PMAA
	η	1	3.8
	τ	0	0
C−R ··· R−C [b]	σ	0	2.0
C−CH_2− ··· −CH_2−C	ω	0	2.3×10^3
C−COOH ··· HOOC−C [c]	ω'	4.7×10^3	4.7×10^3

[a] The group R represents a hydrogen for PAA and a methyl group for PMAA. [b] Energy difference of butane conformations in water.[37] [c] Energy of a hydrogen bond.[36] The results do not depend on the precise values of these two parameters.

experimental titration curves for PAA[35] and PMAA.[34] In both cases, the effective ionization constant pK_{eff} can be fitted quantitatively with the model. The parameters are shown in Table 1.

For PAA, the conformational parameters were fixed to the values $\tau = 0$, $\sigma = 0$, and $\omega = 0$ due to the strong steric repulsions between the corresponding groups, and we take $\eta = 1$ since little interaction is expected. Given of the molecular structure, these values are certainly reasonable. A common value for the two ionization constants was sufficient to obtain a good fitting of the data, whereby the fitted value is $pK_{tt} = pK_{gg} = 4.71$. The best fit pair interaction parameters are $\epsilon = 0.66$ and $\epsilon' = 1.25$.

For PMAA, on the other hand, the hydrophobic attraction between two adjacent methyl groups must be incorporated in the model. While these interactions are absent in PAA, they can be introduced by a nonvanishing parameter σ. Its value has been estimated from energies of butane conformations in water.[37] The parameter τ has been set to zero as for PAA. The ionization constants and the pair interaction parameters were then fitted to the titration data, and one finds $pK_{tt} = 5.33$ and $pK_{gg} = 5.92$ and for the pair interactions we have $\epsilon = 0.70$ and $\epsilon' = 1.5$. In addition, the two parameters η and ω were fitted as well. In contrast to PAA, two different ionization constants to the to conformations must be introduced in order to obtain a good fit of the experimental data. When both constants are assumed to be equal, the conformational transition can be captured qualitatively, but the description of the data remains poor.

The characteristic difference between PAA and PMAA can be explained by the presence of strong attractive interactions between the backbone carbon atoms in the hydrophobic environment. The existence of the different ionization constants can also rationalized due to very different dielectric environment of the carboxylic groups in both conformations.

To characterize the extent of the molecule, we have also evaluated the gyration radius R_g (see Figure 9). The latter quantity can be calculated by the supermatrix techniques developed by Flory[11] as discussed in the Appendix B. We report the gyration radius in the dimensionless form, namely, $R_g^2/(l^2M)$ where l is the bond length and M the number of bonds in the chain. This dimensionless quantity is 1/6 for a freely jointed chain. While the asymptotic limit of a large number of bonds in the molecule M is attained very quickly for the titration curve, the gyration radius converges slowly. The reason probably is that the chain consist of longer helical segments, which basically behave as rigid rods. The latter obey a different scaling of $R_g \propto M$. Nevertheless, the chain is expected to behave Gaussian in the long chain limit due to existing defects.

The available specific viscosity data[14] are also shown in Figure 9 for comparison. For PAA, one observes a gradual variation of both quantities, which is in agreement with model predictions. For PMMA, the model predicts a sharper increase in the gyration radius, but the data indeed suggest a stronger increase of the specific viscosity.[14,15] It should be noted that a different set of viscosity data reports a very sharp transition,[15] quite in accord with the model.

To our knowledge, precise measurements of charging and gyration radii of these polycarboxylic acids of known tacticity are not available at present, and probably the best would be to readdress the problem by analyzing well-characterized samples with titration and scattering techniques. On the other hand, we do not expect that a simple SBRIS description would quantitatively reproduce the gyration radii. The main reason is that long-range interactions are neglected and only short range interactions are taken into account. While this simplification is likely to be appropriate for the description of the protonation, the conformations are surely modified by long-range interactions (i.e., excluded volume effects). The complete picture for the ionization of weak polyelectrolytes will therefore necessitate the consideration of both types of interactions, short-ranged and long-ranged. The best approach would be probably combine the present SBRIS approach to handle the short-range interactions and mean-field models or Monte Carlo simulations to handle the long-range effects.

Despite these shortcomings, to the best of our knowledge it is the first time where a quantitative model is capable of predicting the correct shape of the titration curve of PMAA. Moreover, the parameters entering the present model have very specific molecular meaning. This transition has attracted substantial attention in the soft-matter community and has been compared to a first-order phase transition between the collapsed and extended state.[16,17] However, any quantitative comparison with experimental data was lacking so far. From the present discussion we conclude that the effect can originate from the coupling between protonation of ionizable sites and conformational degrees of freedom of the backbone and seems mainly governed by short-range interactions. However, the detailed interplay between short-ranged and long-ranged interactions is far from being understood. In contrast to attractive van der Waals or hydrophobic interactions, which drive a first-order transition, it will be probably smoothed out by long-ranged repulsive Coulombic forces. The scenario obtained by combining all these effects is far from obvious.

7. Conclusions

Binding of protons to a polyprotic molecule and its conformational degrees of freedom are usually coupled and may lead to nontrivial effects. The most frequent scenario is encountered for noninteracting or repulsive bond−bond interactions. In this case, the proton binding can be described on a contracted level, where the conformational degrees of freedom are averaged out. However, one may encounter attractive (cooperative) interactions between the ionizable sites or higher order interactions, for example, between triplets of sites. An eventual conformational transition is graduate, and its presence cannot be inferred from the titration curve.

The other less frequent but more interesting scenario is that for attractive bond−bond interactions. In this case, the molecule undergoes a sharp conformational transition as a function of pH, and this transition is accompanied by "jump" in the titration curve. While this situation has been related to a first order phase transition, our model predicts this transition to be continuous. The open question remains whether the transition remains continuous or becomes discontinuous in the presence of long-range interactions. While academically interesting, however, this

question is probably of little importance as far one is concerned with real polyelectrolyte systems. Finite size effects are likely to smear out the discontinuities, which might exist in the long chain limit.

Acknowledgment. This research was supported by the Swiss National Science Foundation, the University of Geneva, and by the Spanish Ministry of Education and Science (DGICYT, project BQU2003-9698). Helpful comments by Claude Piguet are gratefully acknowledged.

Appendices

A. Contracting the Four-State SBRIS Model. Consider the four-state SBRIS model defined by the transfer matrix eq 47 in the special case when the binding constants are independent of the conformation. The contracted SB parameters are given by eqs 44, 45, and 46 and they can be obtained analytically with the transfer matrix technique.

The first point to observe is that only the nearest neighbor interaction parameters are nonzero. This point can be demonstrated by inspecting the contraction formulas eqs 45 and 46. To evaluate the nearest neighbor parameters, let us abbreviate them as q_k, where k is the order of the interaction. Thus, $q_2 = \tilde{u}$ are the pair interactions and $q_3 = \tilde{w}$ the triplet interactions. This quantity can be expressed in terms of the recursion relation

$$q_{k+1} = \frac{\langle u_{12}u_{23}...u_{k-1,k}\rangle_c}{q_2^{k-1}q_3^{k-2}...q_k^2} \tag{A.1}$$

for $k \geq 2$. The recursion is initiated with $q_2 = \langle u_{12}\rangle_c$ ($k = 1$).

The evaluation of the interaction parameters is thus reduced to the problem of evaluating the conformational average of a product of pair interaction parameters. This problem is treated in Chapter 4 of Flory's book[11] in detail. For an infinite chain, the sought average can be written as

$$\langle u_{12}u_{23}...u_{k-1,k}\rangle_c = \Xi_c^{-1}\mathbf{q}^T\mathbf{R}^k\mathbf{U}^{N-k-1}\mathbf{p} \tag{A.2}$$

where **U** is the conformational transfer matrix given by eq 24 and **R** is the same matrix, but decorated with the interaction parameters u_g and u_t, namely

$$\mathbf{R} = \begin{bmatrix} u_t & gu_t \\ u_g & ghu_g \end{bmatrix} \tag{A.3}$$

In the infinite chain limit, the averages can be found by evaluating the eigenvalues of the transfer matrices. Denoting the larger and smaller eigenvalues of the matrices **U** and **R** by λ_+, λ_-, ζ_+, and ζ_-, after some algebra we find

$$\langle u_{12}u_{23}...u_{k-1,k}\rangle_c = \frac{\xi_+\eta_-\zeta_-^k - \xi_-\eta_+\zeta_+^k}{\lambda_+^{k-1}(\lambda_+ - \lambda_-)(\zeta_+ - \zeta_-)} \tag{A.4}$$

where $\xi_\pm = \zeta_\pm - u_t - u_g(\lambda_+ - 1)$ and $\eta_\pm = 1 - \lambda_- + (\zeta_\pm - u_t)/u_g$. From this expression, the interaction parameters on the contracted SB level can be evaluated. The resulting titration curves are then found with the transfer matrix technique as discussed in section 2.

B. Radius of Gyration. The calculation of the radius of gyration follows directly Flory's method (Chapter 4 in ref 11). He has shown that the gyration radius R_g can be expressed in a compact fashion as

$$R_g^2 = \frac{2\mathbf{J}^T\mathbf{S}^{M-1}\mathbf{J}'}{M\,\Xi_c} \tag{B.1}$$

where $\mathbf{J}^T = (1, 1, 1, 0, 0, ..., 0)$ and $\mathbf{J}' = (0, 0, ..., 0, 1, 1, 1)^T$ and the supermatrix is

$$\boldsymbol{S} = \begin{bmatrix} \mathbf{U} & \mathbf{U} & (\mathbf{U}\otimes\mathbf{l}^T)\,\|\mathbf{T}\| & (l^2/2)\mathbf{U} & (l^2/2)\mathbf{U} \\ \mathbf{0} & \mathbf{U} & (\mathbf{U}\otimes\mathbf{l}^T)\,\|\mathbf{T}\| & (l^2/2)\mathbf{U} & (l^2/2)\mathbf{U} \\ \mathbf{0} & \mathbf{0} & (\mathbf{U}\otimes\mathbf{E})\,\|\mathbf{T}\| & \mathbf{U}\otimes\mathbf{l} & \mathbf{U}\otimes\mathbf{l} \\ \mathbf{0} & \mathbf{0} & \mathbf{0} & \mathbf{U} & \mathbf{U} \\ \mathbf{0} & \mathbf{0} & \mathbf{0} & \mathbf{0} & \mathbf{U} \end{bmatrix} \tag{B.2}$$

where $\otimes$ is the direct matrix product, **E** the diagonal unit matrix, 0 the zero matrix, and $\mathbf{l}^T = (l, 0, 0)$ the bond row vector. The pseudodiagonal matrix is given by

$$\|\mathbf{T}\| = \begin{bmatrix} \mathbf{T}(\phi_t) & \mathbf{0} & \mathbf{0} \\ \mathbf{0} & \mathbf{T}(\phi_+) & \mathbf{0} \\ \mathbf{0} & \mathbf{0} & \mathbf{T}(\phi_-) \end{bmatrix} \tag{B.3}$$

where the rotational matrixes are defined as

$$\mathbf{T}(\phi^{(\alpha)}) = \begin{bmatrix} \cos\theta & \sin\theta & 0 \\ \sin\theta\cos\phi_\alpha & -\cos\theta\cos\phi_\alpha & \sin\phi_\alpha \\ \sin\theta\sin\phi_\alpha & -\cos\theta\sin\phi_\alpha & -\cos\phi_\alpha \end{bmatrix} \tag{B.4}$$

where θ and ϕ_α represent the dihedral and torsional bond angles for the conformational states $\alpha = t, g^+, g^-$. The formalism can be extended to the case of ionizable chains by the following substitution in eq 1, namely

$$\mathbf{S} \rightarrow \begin{bmatrix} \mathbf{S}_{00} & \mathbf{S}_{01} \\ \mathbf{S}_{10} & \mathbf{S}_{11} \end{bmatrix} \tag{B.5}$$

where $\mathbf{S}_{ij}$ is a supermatrix corresponding to the deprotated ($i, j = 0$) and protonated ($i, j = 1$) states. Thereby, one replaces the corresponding quantities for the protonated and deprotonated sites (cf. eqs 47). The new vectors **J** and **J′** now must be redimensioned accordingly. For example, the row vector **J′** contains 3 ones, 18 zeros, 3 ones, and 18 zeros in sequence. In PAA and PMAA, we have a sequence of different bonds, and thus two different matrixes **S** corresponding to each bond must be used, each of which has to be decorated with the reduced proton activities and interaction parameters as discussed above (cf. eqs 57 and 58).

References and Notes

(1) Steiner, R. F. *J. Chem. Phys.* **1954**, *22*, 1458−1460.
(2) Marcus, R. A. *J. Phys. Chem.* **1954**, *58*, 621−623.
(3) Katchalsky, A.; Mazur, J.; Spitnik, P. *J. Polym. Sci.* **1957**, *23*, 513−532.
(4) Borkovec, M.; Daicic, J.; Koper, G. J. M. *Proc. Natl. Acad. Sci. U.S.A.* **1997**, *94*, 3499−3503.
(5) Ullner, M.; Jonsson, B. *Macromolecules* **1996**, *29*, 6645−6655.
(6) Borkovec, M.; Jönsson, B.; Koper, G. J. M. In *Surface and Colloid Science*; Matijević, E., Ed.; Plenum Press: New York, 2001; Vol. 16.
(7) Borkovec, M.; Koper, G. J. M. *J. Phys. Chem.* **1994**, *98*, 6038.
(8) Koper, G. J. M.; van Duijvenbode, R. C.; Stam, D. D. P. W.; Steuerle, U.; Borkovec, M. *Macromolecules* **2003**, *36*, 2500−2507.
(9) Kesvatera, T.; Jonsson, B.; Thulin, E.; Linse, S. *Proteins* **2001**, *45*, 129−135.
(10) Felemez, M.; Bernard, P.; Schlewer, G.; Spiess, B. *J. Am. Chem. Soc.* **2000**, *122*, 3156−3165.
(11) Flory, P. L. *Statistical Mechanics of Chain Molecules*; John Wiley: New York, 1969.
(12) Vacatello, M.; Flory, P. J. *Macromolecules* **1986**, *19*, 405−415.
(13) Yoon, D. Y.; Suter, U. W.; Sundararajan, P. R.; Flory, P. J. *Macromolecules* **1975**, *8*, 784−789.

(14) Sakurai, M.; Imai, T.; Yamashita, F.; Nakamura, K.; Komatsu, T.; Nakagawa, T. *Polym. J.* **1993**, *25*, 1247−1255.
(15) Katchalsky, A.; Eisenberg, H. *J. Polym. Sci.* **1950**, *6*, 145−154.
(16) Raphael E.; Joanny J. F. *Europhys. Lett.* **1990**, *13*, 623−628.
(17) Uyaver, S.; Seidel, C. *Europhys. Lett.* **2003**, *64*, 536−542.
(18) Uyaver, S.; Seidel, C. *J. Phys. Chem. B* **2004**, *108*, 18804−18814.
(19) Castelnovo, M.; Sens, P.; Joanny, J. F. *Eur. Phys. J. E* **2000**, *1*, 115−125.
(20) Poland, D.; Scheraga, H. A. *Theory of Helix−Coil Transitions in Biopolymers*; Academic Press: New York, 1970.
(21) Olander, D. S.; Holtzer, A. *J. Am. Chem. Soc.* **1968**, *90*, 4549−4560.
(22) Nishio, T. *Biophys. Chem.* **1998**, *71*, 173−184.
(23) Figueirido, F.; Del Buono, G. S.; Levy, R. M. *J. Phys. Chem.* **1996**, *100*, 6389−6392.
(24) Ben-Naim A. *J. Chem. Phys.* **1998**, *108*, 3630−3647.
(25) Ben-Naim, A. *J. Chem. Phys.* **1998**, *109*, 7443−7449.
(26) Noszal, B.; Sandor, P. *Anal. Chem.* **1989**, *61*, 2631−2637.
(27) Noszál, B. In *Biocoordination Chemistry*; Burger, K., Ed.; Ellis Horwood: New York, 1990.
(28) Smits, R. G.; Koper, G. J. M.; Mandel, M. *J. Phys. Chem.* **1993**, *97*, 5745−5751.
(29) Koper, G. J. M.; Borkovec, M. *J. Chem. Phys.* **1996**, *104*, 4204−4213.
(30) Ising, E. *Z. Phys.* **1925**, *31*, 253−258.
(31) Robertson, H. S. *Statistical Thermophysics*: Prentice Hall: Englewood Cliffs, NJ, 1993.
(32) Wyman, J.; Gill, S. J. *Binding and Linkage*; University Science Books: Mill Valley, CA, 1990.
(33) Perlmutter-Hayman, B. *Acc. Chem. Res.* **1986**, *19*, 90−96.
(34) Nagasawa, M.; Murase, T.; Kondo, K. *J. Phys. Chem.* **1965**, *69*, 4005−4012.
(35) Kawaguchi, Y.; Nagasawa, M. *J. Phys. Chem.* **1969**, *73*, 4382−4384.
(36) Atkins, P. *Physical Chemistry*; W. H. Freeman: New York, 1997.
(37) Ashbaugh, H. S.; Kaler, E. W.; Paulaitis, M. E. *Biophys J.* **1998**, *75*, 755−768.